JOURNAL OF GEOPHYSICAL RESEARCH, VOL. 99, NO. A1, PAGES 159–167, JANUARY 1, 1994

Dispersion and wave coupling in inhomogeneous MHD waveguides

Andrew N. Wright

Department of Mathematical and Computational Sciences, University of St. Andrews, Fife, Scotland

The propagation of the fast mode is considered in nonuniform waveguides. We show how the natural dispersion inherent in a waveguide will select waveguide modes with a small wavenumber (k_y) along the guide to remain near a localized source region of fast mode energy. It is these modes that are shown to have a coherent periodic time dependence over many cycles that are suitable for driving observable Alfvén resonances (magnetic pulsations). We expect the frequencies of Alfvén resonances to be very close to the eigenfrequencies of waveguide modes with $k_y = 0$.

1. Introduction

The coupling of different MHD wave modes in inhomogeneous media is of interest to laboratory, space, and solar plasma physicists. In particular the resonant coupling of fast and Alfvén waves may be important for heating laboratory fusion plasmas and the corona of the sun. Such resonant coupling is thought to be important for understanding ULF magnetic pulsations in the Earth's magnetosphere [*Southwood*, 1974; *Chen and Hasegawa*, 1974]. The in situ observations of pulsations afforded by satellite instruments and ground-based radar permit a detailed examination of the coupling process.

In this paper we shall consider resonant coupling in the magnetospheric context, although our results will be of relevance to other areas. The history of modeling ULF waves in the magnetosphere dates back to the decoupled wave mode studies of *Dungey* [1954,1967], which form the basis of coupled mode calculations [*Wright*, 1992*a*]. For the fast mode to drive an Alfvén resonance it must have a periodic time dependence with a well-defined frequency. The mechanism through which an oscillatory fast mode may be established in the magnetosphere has been discussed for two decades: Initially it was suggested that the Kelvin-Helmholtz instability at the magnetopause was the origin of the fast mode [*Southwood*, 1974; *Chen and Hasegawa*, 1974]. Subsequently, the cavity mode model was developed [*Kivelson and Southwood*, 1985; *Allan et al.*, 1986; *Lee and Lysak*, 1989] in which the magnetosphere reverberates with the natural fast modes of the magnetospheric cavity. The most recent ideas modify the cavity model and treat the magnetosphere as an open-ended waveguide [*Samson et al.*, 1992].

In the cavity model the wavenumber around the cavity (i.e., in azimuth) takes on discrete values, and consequently the natural frequencies of the fast cavity modes also adopt discrete values. In contrast the waveguide model has a continuous range of wavenumbers along the waveguide (i.e., around the dayside and into the magnetotail), and the fast waveguide modes have a correspondingly continuous spectrum. The discrete frequency spectrum of the fast cavity modes is suitable for driving a series of Alfvén resonances; however, it is not obvious that the continuous frequency spectrum of the fast waveguide modes will be able to drive resonances at discrete frequencies. *Walker et al.* [1992] addressed this issue: they considered a disturbance moving along the outer boundary of the waveguide and argued that only fast modes with a small wavenumber along the waveguide would be excited. Thus we have a discrete value of wavenumber and a discrete fast mode frequency spectrum. *Harrold and Samson* [1992] considered the modes of an extended waveguide in which the bow shock was the outer boundary. In their model they assumed a constant wavenumber along the waveguide, which may be valid if the solar wind has a dominant wavenumber. (It is unlikely that the mechanism suggested by *Walker et al.* [1992] will be important if the outer boundary is the bow shock, since material is free to pass through this boundary, and will not have to move along it.)

The magnetospheric waveguide model is still in its infancy, being proposed and developed in a few recent papers [*Samson et al.*, 1992; *Walker et al.*, 1992; *Harrold and Samson*, 1992]. In this paper we develop concepts that give some idea of the type of behavior we should expect in MHD waveguides. In particular we address the problem of how the waveguide may excite discrete resonances. Our approach is complementary to those adopted to date: rather than drive the waveguide continually from its outer boundary, we simply assume that some fast mode energy enters the waveguide and ask how it will evolve. We develop the concept of dispersion in MHD waveguides, and demonstrate how this will naturally favor fast modes with a small wavenumber along the waveguide as being most important for driving Alfvén resonances.

The paper is structured as follows: section 2 introduces the model and governing equations; section 3 reviews the basic properties of uniform waveguides followed by a treatment of their dispersive behavior in section 4; section 5 address the dispersion of fast mode disturbances in nonuniform waveguides, and section 6 discusses how the fast mode may couple to the Alfvén mode. Finally, section 7 summarizes the main points of the paper.

2. Governing Equations

The model we adopt for studying wave propagation in a waveguide is to take the magnetospheric box model [*Southwood*, 1974] used in cavity model studies, but allow the box

Paper number 93JA02206.
0148-0227/94/93JA-02206$05.00

to have an infinite length with no imposed periodicities in this direction. We can think of the open-ended waveguide as extending from the noon magnetosphere around the dawn and dusk flanks then on into an infinitely long magnetotail (see Figure 1*a*). Figure 1*b* shows half of the waveguide extending from noon into the magnetotail. We have retained the traditional box coordinates in which x measures the distance across the waveguide/cavity, y is the distance along the waveguide, and z is the field-aligned coordinate.

We assume the background magnetic field $\mathbf{B}$ to be uniform, but allow the plasma density to vary in the (x, y) plane. The waveguide width extends from $x = 0$ near the Earth to the outer boundary at $x = x_m$. In the studies by *Samson et al.* [1992] and *Walker et al.* [1992] the outer boundary was taken to be the magnetopause, while *Harrold and Samson* [1992] took this boundary to be the bow shock. The general ideas put forward in this paper rely upon having efficient reflecting boundaries at $x = 0$ and x_m, and are independent of whether x_m corresponds to the magnetopause or the bow shock. For simplicity we assume the plasma to have a low β, so our model approximates magnetospheric plasma better than the magnetosheath plasma. Neglecting resistivity, the governing equations for the linear plasma displacement (ξ) and the compressional magnetic field (b_z) perturbations are

$$\frac{1}{V^2}\frac{\partial^2 \xi_x}{\partial t^2} - \frac{\partial^2 \xi_x}{\partial z^2} = -\frac{1}{B}\frac{\partial b_z}{\partial x} \tag{1}$$

$$\frac{1}{V^2}\frac{\partial^2 \xi_y}{\partial t^2} - \frac{\partial^2 \xi_y}{\partial z^2} = -\frac{1}{B}\frac{\partial b_z}{\partial y} \tag{2}$$

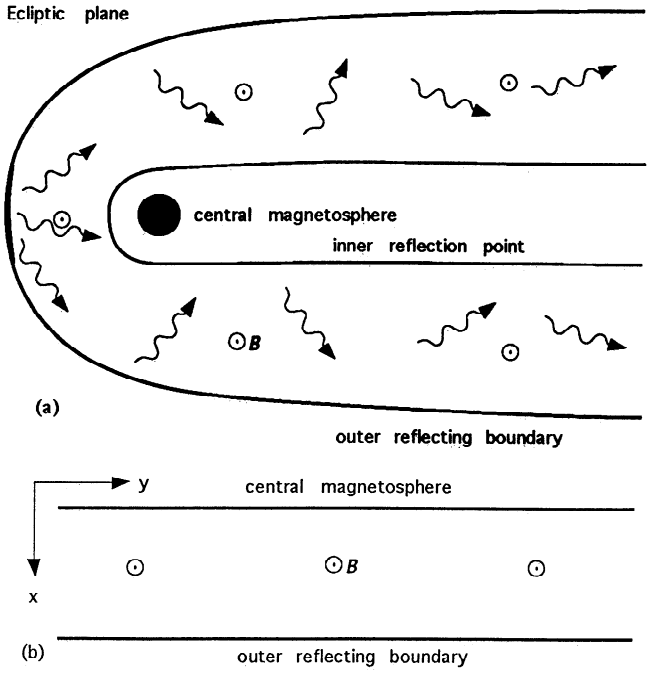

Fig. 1. (*a*) The magnetospheric waveguide viewed in the ecliptic plane. Fast mode waves (depicted as wiggly arrows) enter the waveguide and subsequently suffer reflection from an outer boundary (perhaps the magnetopause or the bow shock) and an inner reflection point (the plasmapause or a "turning point"). (*b*) Half of the waveguide (from noon, around the dusk flank and into the magnetotail) is approximated as an infinitely long waveguide containing a uniform magnetic field and plasma whose density depends on x and y.

$$b_z = -B\left(\frac{\partial \xi_x}{\partial x} + \frac{\partial \xi_y}{\partial y}\right) \tag{3}$$

where $V = B/\sqrt{\mu_0 \rho}$ is the local Alfvén speed, and ρ the plasma density.

The growth of any Alfvén resonance will manifest itself in the ξ_y plasma displacement. It is evident from (2) that the magnetic pressure gradient of the fast mode (Bb_z/μ_0) in the $\hat{\mathbf{y}}$ direction will be responsible for driving the resonance, so it is important to determine the how the fast mode evolves.

3. Uniform Waveguides

To study the nature of fast waves in a waveguide we consider a particularly simple system first, namely, a uniform waveguide in which ρ and V are constant. In such a medium the governing equations above may be combined in a single wave equation for the fast mode perturbation b_z,

$$\frac{\partial^2 b_z}{\partial t^2} = V^2\left(\frac{\partial^2}{\partial x^2} + \frac{\partial^2}{\partial y^2} + \frac{\partial^2}{\partial z^2}\right) b_z \equiv V^2 \nabla^2 b_z \tag{4}$$

Consider normal modes of the waveguide of the form $\exp i(\omega t \pm \mathbf{k}\cdot\mathbf{r})$, where ω is the frequency of the mode, $\mathbf{k} = (k_x, k_y, k_z)$ is the wavevector, and $\mathbf{r} = (x, y, z)$. Substitution of this dependence into (4) yields the dispersion relation for the fast mode,

$$\omega^2 = V^2\left(k_x^2 + k_y^2 + k_z^2\right) \tag{5}$$

In an infinite medium this relation gives nondispersive propagation. However, in a waveguide the boundary conditions in the x and z directions restrict the choice of wavenumbers and introduce dispersion. Suppose that the boundaries in x are perfectly reflecting (e.g., $\xi_x = \partial b_z/\partial x = 0$), as are those in z ($\xi_x = \xi_y = b_z = 0$) which represent the ionospheric boundary for closed field lines. Then

$$k_x = \pm n\pi/x_m \quad k_z = \pm m\pi/z_m \quad n, m = 1, 2, 3... \tag{6}$$

where z_m is the length of the field lines.

Given the values of k_x and k_z, we may use (6) to find k_y as a function of ω,

$$k_y^2 = \frac{\omega^2}{V^2} - k_x^2 - k_z^2 \equiv \frac{\omega^2}{V^2} - \frac{\omega_c^2}{V^2} \tag{7}$$

where $\omega_c^2 = V^2(k_x^2 + k_z^2)$ is the waveguide cuttoff frequency of the (n, m) mode familiar in electrical and acoustic waveguides. If $\omega^2 > \omega_c^2$, k_y is real and the mode may propagate along the guide. If $\omega^2 < \omega_c^2$, k_y is imaginary and the mode is evanescent along the waveguide, prohibiting propagation.

If we believe that the boundary at x_m is not a reflector but is driven, it is more appropriate to impose a wavenumber k_y along the outer boundary and solve for k_x. This is the case when the magnetopause is driven by the Kelvin-Helmholtz instability. In this situation k_x is found to be imaginary, and the mode is evanescent in x.

4. Dispersion in Uniform Waveguides

The dispersive nature of waveguide propagation may be illustrated clearly in a two-dimensional waveguide. This is achieved by setting $k_z = 0$ so that the waves propagate in the x and y directions, but not in z. Fast modes could be established in the waveguide as a result of a density enhancement in the solar wind striking the outer boundary at some location. It is likely that fast mode waves will propagate

from this location into the body of the waveguide. Figure 2*a* shows the fast mode inside the waveguide shortly after excitation from the boundary has stopped. We now treat the boundaries in x as perfectly reflecting and study the subsequent propagation. The evolution of the fast mode may be described in terms of either propagating wavepackets or the group velocities associated with various waveguide modes. We shall consider both in this section, but begin with the former, which is easier to interpret physically.

Ray Trajectories

In a uniform medium the fast mode disturbance of Figure 2*a* may be decomposed into a series of propagating plane wavepackets. The wavevector of any plane wave is perpendicular to the plane wavefronts (and confined to the plane $z = \text{const}$, since $k_z = 0$). The trajectory of a wavepacket is calculated by allowing it to move in the direction of its wavevector at the local Alfvén speed. When the wavepacket encounters one of the reflecting boundaries, the normal component of the wavevector changes sign. By continuing this procedure the "ray trajectory" of the wavepacket may be found. Figure 2*b* shows the ray trajectories of three wavevectors, along with an observer (O) a distance y_0 down the waveguide.

The qualitative behavior of the system is straightforward: The ray with wavevector k_1 aligned with the $\hat{\mathbf{y}}$ direction will propagate straight out of the waveguide through O without reflecting off the boundaries. If this ray leaves the source region at time $t = 0$, then it will reach O at $t = y_0/V$. The ray k_2 will suffer one reflection on its journey to O and has a slightly longer path length than the ray k_1. Consequently, it will arrive at O later than the k_1 ray. Finally, the ray k_3 propagates across the waveguide and shuffles down its length very slowly. This ray will take a long time to reach O.

From the simple description above it is apparent that we shall have dispersion in both space and time: The waves at a given instant in time will have dispersed spatially with the largest k_y/k_x ratio wavepackets furthest down the waveguide and the smaller k_y/k_x ratio wavepackets correspondingly nearer to the source. Alternatively, consider the waves seen at a given point in space (say, O) as a function of time:

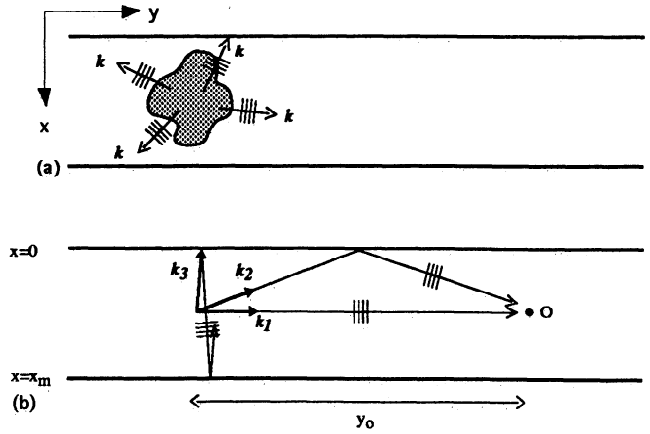

Fig. 2. (*a*) A source of fast mode waves is present inside the waveguide (shaded region). The source may be decomposed into a sum of propagating plane wavepackets with wavevectors $\mathbf{k}$. (*b*) The trajectories of three wavepackets propagating away from the source region and along the waveguide.

The largest k_y/k_x ratio waves are seen at the earliest time, followed by wavepackets with smaller k_y/k_x at later times, i.e., dispersion in time.

We may quantify these ideas by considering the time of flight of different rays from the source to O. The first waves to arrive at O when $t = y_0/V \equiv t_0$ are those with $\mathbf{k} = (0, k_y, 0)$. The actual value of k_y depends upon the stucture of the source of waves. A wave leaving the center of the source region and bouncing off the boundaries j times will traverse a distance in x of jx_m. From the orientation of this ray, which is aligned with $\mathbf{k}$, it is evident that

$$\frac{y_0}{jx_m} = \frac{k_y}{k_x} \tag{8}$$

The time taken for the ray to reach O is

$$t = \sqrt{y_0^2 + j^2 x_m^2}/V \tag{9}$$

Combining (8) and (9) with the minimum transit time $t_0 = y_0/V$, we find k_y at O as a function of time,

$$\frac{k_y^2(y_0,t)}{k_x^2(y_0,t)} = \frac{1}{t^2/t_0^2 - 1} \qquad t > t_0 \tag{10}$$

After a few periods of t_0 we may approximate (10) by

$$k_y(y_0,t) \approx k_x \cdot \frac{t_0}{t} \qquad t \gg t_0 \tag{11}$$

which suggests that the value of k_y seen at $y = y_0$ will tend to zero for large times on a time scale of t_0. Near the source of waves ($t_0 \approx y_0 \approx 0$) the value of k_y observed will tend to zero very rapidly, as one would expect, since waves with a significant k_y will soon propagate away.

We may also derive the frequency of the waves observed at O as a function of time. The dispersion relation (5) gives the frequency in terms of the wavenumbers. Recalling that we have set $k_z = 0$ and employing (10), we find

$$\omega^2(y_0,t) = k_x^2 V^2 \left(1 + \frac{1}{t^2/t_0^2 - 1}\right) \qquad t > t_0 \tag{12}$$

Evidently the frequency of the wave seen at O tends to $k_x V$ for t greater than a few times t_0, which is just the low k_y limit we would anticipate from (11).

It is possible to see these features in a simple numerical solution of the waveguide equations: We assume the source of fast waves to be centered on $(\frac{1}{2}x_m, 0)$ and have $k_z = 0$ again. The source is symmetric about the $\hat{\mathbf{z}}$ direction and will propagate radially outward according to

$$b_z(x,y,t) \approx \phi(R - Vt)/\sqrt{R} \tag{13}$$

in an unbounded medium, where R is the distance from the center of the source region. The reflection from boundaries in x is accommodated by having image sources along the line $y = 0$ so that $\partial b_z/\partial x = 0$ at $x = 0, x_m$. The properties of the solution are not very sensitive to the function ϕ. For the results shown here we took b_z at $t = 0$ to be zero at $R = 0$ and $x_m/2$, and to have a negative then positive value between (b_z and its first derivative are continuous throughout). The profile of b_z is shown in Figure 4*a*.

Figure 3 shows contours of b_z in the (x, y) plane for the times $t = 0, 4, 10$ in a waveguide of length 12. (Distances, velocities, and times are normalized by x_m, V, and x_m/V, respectively.) The initial b_z disturbance in figure 3(a) propagates and relaxes to the states shown in 3(b,c) at later times: the system is not driven, and the boundaries are perfectly

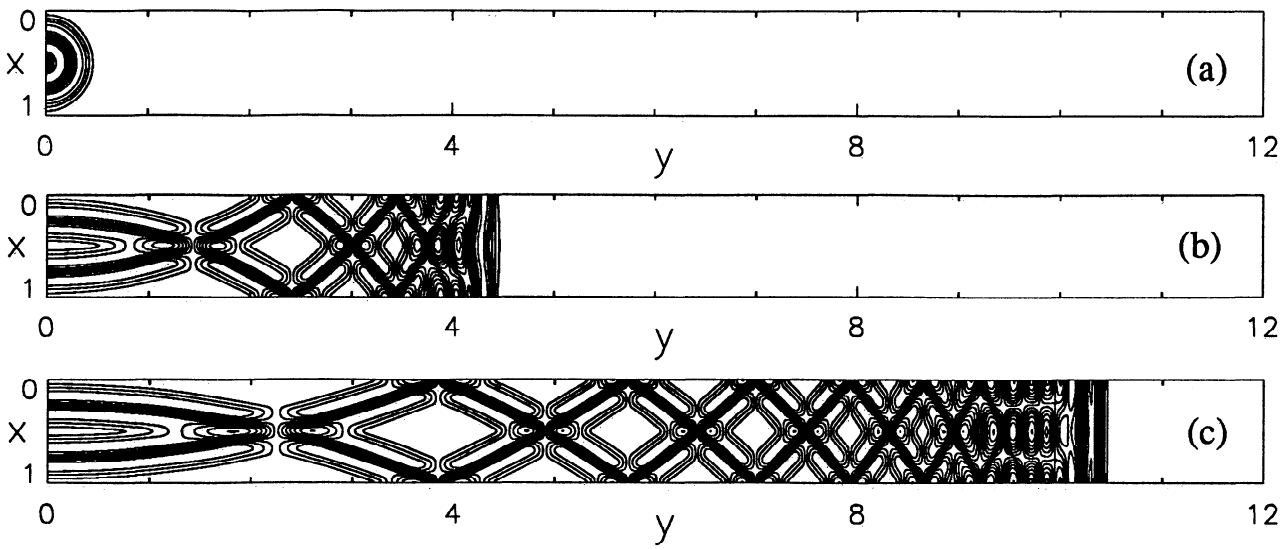

Fig. 3. Contour plots of b_z. (a) The initial circular distribution of fast mode waves at $t = 0$, with a contour interval of 0.426. (b) When $t = 4$ the waves have propagated along the guide with waves near $y = 4.5$ propagating directly out of the guide (i.e., $\mathbf{k}$ aligned with $\hat{\mathbf{y}}$) and waves near $y = 0$ propagating across the guide (i.e., $\mathbf{k}$ aligned with $\hat{\mathbf{x}}$). The contour interval is 0.136. (c) At $t = 10$ the waves have reached a distance $y = 10.5$ along the waveguide. Now the wavefronts at $y = 4.5$ tend to propagate across the guide rather than along it as in Figure 3(b). The contour interval is 0.078.

reflecting. Note how the leading wavefront running out of the guide has a wavevector aligned with $\hat{\mathbf{y}}$, as expected. Also the wavefronts at a given y propagate increasingly in the $\hat{\mathbf{x}}$ direction at later times (i.e., k_y becomes smaller). Figure 4 shows the variation of b_z along the center line of the waveguide $(\frac{1}{2}, y)$ for the same times presented in Figure 3. Its dispersion in space is manifested by fine structure (large k_y) in the leading edge and larger scales (smaller k_y) nearer the source.

The frequency of the b_z perturbation observed at a fixed position may be investigated by considering the time variation of b_z at that point. Figures 5a and 5b display $b_z(t)$ at $(\frac{1}{2}, 0)$ and $(\frac{1}{2}, 1)$, repectively. For the point $(\frac{1}{2}, 0)$, t_0 is zero, and the wave settles down immediately to having a period of 1 as suggested by (12). (The period of 1 corresponds to the fundamental waveguide mode in x with $k_y = 0$.) For the point at $(\frac{1}{2}, 1)$ we find $t_0 = 1$. Initially $b_z(\frac{1}{2}, 1, t)$ oscillates with a short period, which subsequently tends to the value 1 on a time scale of t_0 (in accord with (12)).

It is interesting to note that the amplitude of b_z in Figure 5 decays with time. Physically, this is attributable to the decreasing energy density near the source as fast mode continually leaks down the waveguide. Mathematically, we can interpret the feature as follows: At time t the disturbance in the waveguide (at $(\frac{1}{2}, 0)$) will have come from an image source a distance t along the y axis (in normalized units). From the form of the wave in (13) it is apparent that the amplitude of this disturbance will decrease in time as $1/\sqrt{t}$. Similar ideas may be used to understand the amplitude variations in Figure 4.

Waveguide Normal Modes

A complementary view of the propagation of disturbances within the waveguide is to consider the group velocities of the waveguide modes. The waveguide modes form a complete orthogonal set of functions; thus we may construct any initial disturbance as a sum over these functions and study the subsequent evolution mode by mode. (This sum would take the form of a Fourier series in the x and z directions, and a Fourier integral in the y direction.)

In this subsection we shall allow the modes to have a wavenumber in z, $\mathbf{k} = (k_x, k_y, k_z)$, and look for solutions of the form $\exp i[\omega t \pm \mathbf{k} \cdot \mathbf{r}]$. These modes have the dispersion relation (5) in a uniform medium, k_x and k_z being quantized according to (6). Since we are interested primarily in propagation along the waveguide (i.e., in the $\hat{\mathbf{y}}$ direction) we shall define V_p and V_g to be the phase and group velocities along $\hat{\mathbf{y}}$. Employing (5) gives, for waves propagating in the $+\hat{\mathbf{y}}$ direction,

$$V_p = \frac{\omega}{k_y} = \frac{k}{k_y} V \tag{14a}$$

$$V_g = \frac{\partial \omega}{\partial k_y} = \frac{k_y}{k} V \tag{14b}$$

which yields the familiar waveguide relation

$$V_p V_g = V^2 \tag{15}$$

The rate at which a waveguide mode transports energy and information in the $\hat{\mathbf{y}}$ direction is given by V_g. From (14b) we find agreement with our expectations based on ray trajectories: Those modes with $k_y^2 \ll k_x^2$ and k_z^2 have $V_g \approx 0$ and transport no energy along $\hat{\mathbf{y}}$; Those modes with $k_y^2 \gg k_x^2$ and k_z^2 have $V_g \approx V$, and transport energy at the local Alfvén speed in $\hat{\mathbf{y}}$.

We may also derive the dispersive properties of the waveguide shown in Figure 2 in terms of the waveguide modes. The general source of waves in Figure 2a may be decomposed into waveguide modes as described above. The first modes to reach the point O in Figure 2b will be those with a group velocity equal to V aligned with $\hat{\mathbf{y}}$, i.e., the modes with $k_y^2 \gg k_x^2$ and k_z^2. These modes will arrive when $t = t_0 \equiv y_0/V$. At subsequent times t the modes at O will have wavenumbers determined by the condition $V_g(k)t = y_0$. Using (14b) to re-express this condition, we find

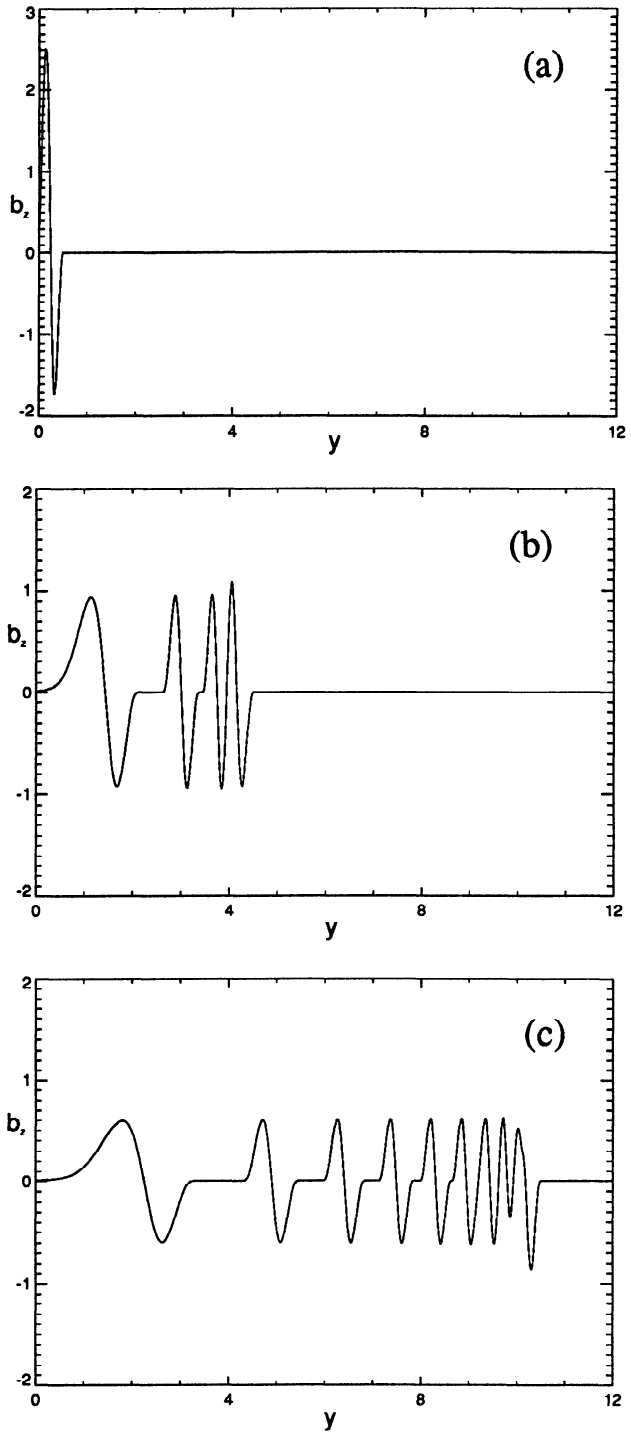

Fig. 4. Snapshots of the variation of b_z along the center line of the waveguide ($x/x_m = \frac{1}{2}, y$) for (a) $t = 0$, the initial source, (b) $t = 4$, and (c) $t = 10$. These plots correspond to those shown in Figure 3. Note the decreasing amplitude of b_z at later times, and the way that fine structure (large k_y) is always present in the leading edge while larger scales in b_z (smaller k_y) develop at smaller y as time increases.

$$k_y^2(y_0, t) = \frac{k_x^2 + k_z^2}{t^2/t_0^2 - 1} \tag{16}$$

for $t > t_0$. (Setting $k_z = 0$ recovers the two-dimensional result (10).) Similarly, we may find the frequency of the signal at O from the dispersion relation (5) and (16),

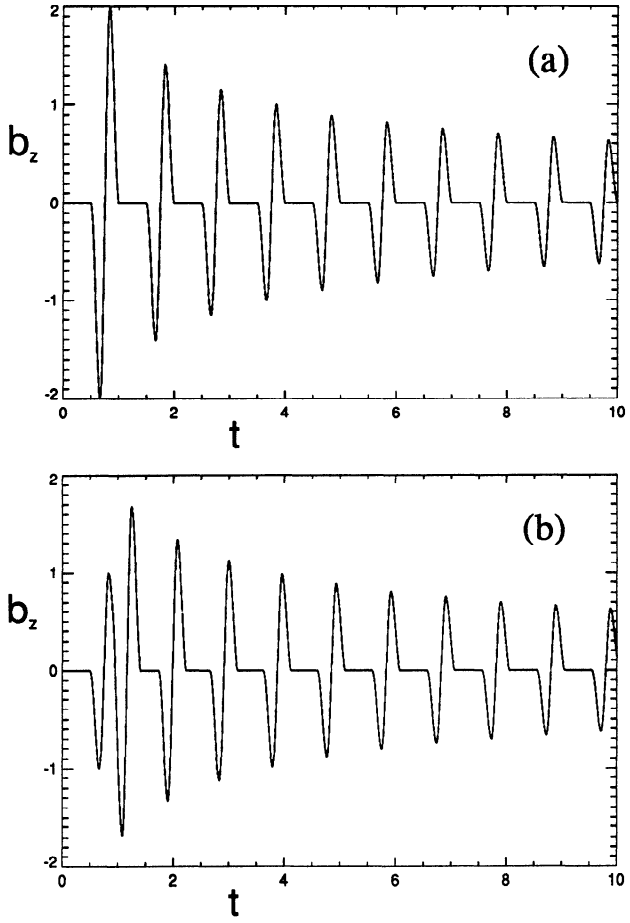

Fig. 5. The time variation of b_z at the points (a) $(\frac{1}{2}, 0)$, and (b) $(\frac{1}{2}, 1)$. The time period of waves at $(\frac{1}{2}, 0)$ is the fundamental period 1, and the amplitude varies as $1/\sqrt{t}$. Dispersion is observed in the variation of b_z at $(\frac{1}{2}, 1)$ and manifests itself in the high-frequency oscillation initially observed which then tends to the fundamental period 1.

$$\omega^2(y_0, t) = (k_x^2 + k_z^2)V^2 \left(1 + \frac{1}{t^2/t_0^2 - 1}\right) \qquad t > t_0 \tag{17}$$

which again generalizes the two-dimensional result (12). After a few time scales t_0 we find that the solution has the following limit,

$$k_y \to 0 \qquad \omega^2 \to (k_x^2 + k_z^2)V^2 \tag{18}$$

so the frequency tends to the $k_y = 0$ cavity mode frequency. This effect may be observed in acoustic waveguides such as an alley between two buildings. Stamping your foot in the middle of the alley excites a broad spectrum of wavenumbers; however, the only sound waves you will hear are the ones that stay near you, i.e., the waves with a wavevector directed across the alley. For example, an alley of width 3 m should reverberate with a frequency of about 50 Hz.

5. DISPERSION IN INHOMOGENEOUS WAVEGUIDES

The previous section has explained the idea of dispersion in a uniform waveguide. In this section we develop the more complicated idea of dispersion in nonuniform waveguides, which must be employed for a sensible discussion of magnetospheric waveguides. We shall let the Alfvén speed decrease monotonically with x as appropriate to the Earth's magne-

tosphere, and assume the background to be independent of y and z. (Note that we shall assume the magnetic field to be uniform and allow the density to vary with x.) The inhomogeneous medium means that the fast and Alfvén modes will now be coupled together, and the possibility of resonant excitation must be considered, especially as section 4 showed how the dispersive nature of the waveguide will permit the fast mode to oscillate at a single steady frequency. For the moment we shall develop the normal mode description, and then consider ray trajectories.

Waveguide Normal Modes

The inhomogeneity in x means that we can only consider Fourier components in the y and z directions. Seeking normal modes of the form $b_z(x)\exp i[\omega t \pm k_y y \pm k_z z]$, the governing equations (1)-(3) yield the following familiar equation for b_z,

$$\frac{d^2 b_z}{dx^2} - \frac{\omega^2 dV^{-2}/dx}{\omega^2/V^2 - k_z^2}\cdot\frac{db_z}{dx} + \left(\frac{\omega^2}{V^2} - k_y^2 - k_z^2\right) b_z = 0 \quad (19)$$

Solving this equation for given boundary conditions in x yields a set of orthogonal eigenfunctions $b_z(x)$ and eigenfrequencies, which may be used to synthesize the profile in x of the initial disturbance [*Barston*, 1964].

The general behavior of this equation has been discussed in depth in the context of cavity modes [*Kivelson and Southwood*, 1985; *Kivelson and Southwood*, 1986; *Inhester*, 1987; *Walker et al.*, 1992]. The main features of the solution are as follows: A singularity occurs at the position x_r where

$$\omega^2 = k_z^2 V^2(x_r) \quad (20)$$

In terms of a WKB description, the solution for b_z has a turning point at x_t defined via

$$\omega^2 = \left(k_y^2 + k_z^2\right) V^2(x_t) \quad (21)$$

In the low Alfvén speed region (x between $[x_t, x_m]$) the fast mode may propagate, while in the high Alfvén speed region $[0, x_t]$ the mode is evanescent. Thus the resonant singularity, x_r, is in the evanescent tail of the fast mode. The second term in (19) dominates near x_r, but is small in the propagating interval. This is particularly true in the WKB limit where we consider waves of short wavelength in x; i.e., second derivatives of b_z are much greater than first derivatives. Accordingly, in the lowest-order WKB analysis we may neglect the second term and solve the following reduced wave equation in the propagation region [*Inhester*, 1987]:

$$\frac{d^2 b_z}{dx^2} + \left(\frac{\omega^2}{V^2} - k_y^2 - k_z^2\right) b_z = 0 \quad (22)$$

We see that the effective local wavenumber in x is given by

$$k_x^2(x,\omega) = \frac{\omega^2}{V^2(x)} - k_y^2 - k_z^2 \quad (23)$$

and note that k_x is now an explicit function of x through the nonuniformity of the Alfvén speed, $V(x)$. The Bohr-Sommerfeld (or phase integral) condition which the wave must satisfy is [*Bender and Orszag*, 1978]

$$\int_{x_t}^{x_m} k_x(x)dx = (n+\alpha)\pi \qquad n = 1, 2... \quad (24)$$

the phase factor α is determined by the boundary conditions in x. For a perfect reflector at x_m, ($\xi_x = 0$), and evanescent decay at small x we find $\alpha = -1/4$ [*Walker et al.*, 1992]. If there is a resonance in the waveguide, this will modify α; however, since the resonance will be in the evanescent tail there would be no leading order change in α.

Equation (24) is an integral relation for the eigenfrequencies of the fast mode: We specify k_y, k_z, and n (the number of the mode in x), then find the nth eigenfrequency as that frequency for which the criterion (24) is met.

To illustrate the character of the solutions we have calculated the dispersion diagram $\omega(k_y, n)$ for the Alfvén speed variation $V = V_0(1 - x/x_0)$. (This functional form was chosen because it yields an integrable phase relation.) Quantities are normalized by the dimension x_m and speed at $x = 0$, V_0. We chose the Alfvén speed to vary from 100 km/s at $x_m = 15\ R_E$ to 2000 km/s near the plasmapause $x = 5\ R_E$ (e.g., *Harrold and Samson* [1992]). Hence the scale length of the background medium is $x_0 = 295/19\ R_E$ and $V_0 = 2950$ km/s. The length of the field lines in z is taken to be $2x_m$. Figure 6 displays the dispersion relation for the fundamental mode in z; $k_z = \pi/2x_m$. The curves correspond to the first two harmonics in x, the lowest being the fundamental ($n = 1$). The quantity Ω_n is defined to be $\omega_n x_m/V_0$.

Figure 6 may be interpreted as follows: For a specific harmonic of the waveguide mode (i.e., n) we may read off the frequency ω_n of the mode given a value of k_y. The curve contains information about the phase and group velocities: The phase velocity is simply ω_n/k_y, whereas the group velocity of the mode is the gradient of the line, $\partial\omega_n/\partial k_y$.

Analytical expressions may be obtained for the phase and group velocity of a mode. Following *Walker et al.* [1992] we substitute (23) into (24), and differentiating with respect to k_y (assuming α to be a constant) we find a modified waveguide relation (cf. equation (15))

$$\frac{\omega}{k_y}\cdot\frac{\partial\omega}{\partial k_y} \equiv V_p V_g = \langle V^{-2}\rangle^{-1} \quad (25a)$$

where

$$\langle V^{-2}\rangle = \int_{x_t}^{x_m} V^{-2} k_x^{-1} dx \Big/ \int_{x_t}^{x_m} k_x^{-1} dx \quad (25b)$$

rearranging for the group velocity we find

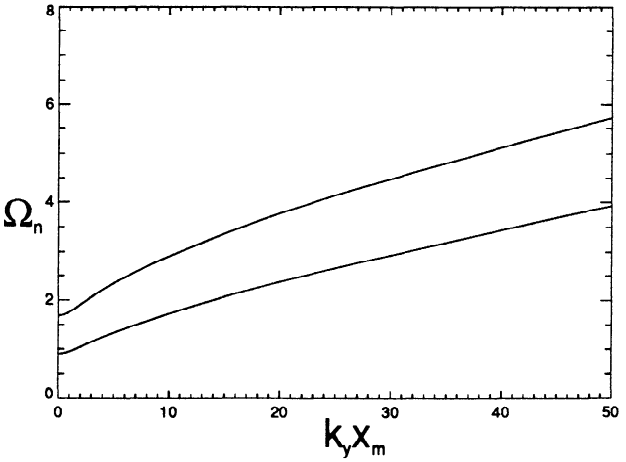

Fig. 6. The dispersion diagram for the first two modes of the inhomogeneous waveguide ($n = 1$ being the lowest curve).

$$V_g = \frac{\partial \omega}{\partial k_y} = \frac{k_y}{\omega}\langle V^{-2}\rangle^{-1} \tag{26}$$

From (26) it is evident that the result found for the uniform waveguide of V_g being zero when $k_y = 0$ is still valid for inhomogeneous waveguides. This property is manifested in Figure 6 by the gradient of the dispersion curves in Figure 6 being zero when $k_y = 0$.

Another property deduced for the uniform waveguide was that of greatest group velocity for modes with the greatest value of k_y/k (14b). This, in fact, is not the case in a nonuniform waveguide and would require the gradients of the curves in Figure 6 to monotonically increase with k_y. It is easiest to interpret the variation of group velocity with k_y in terms of ray trajectories, to which we now turn.

Ray Trajectories

The trajectory of a wavepacket with wavenumber $\mathbf{k}$ is given by

$$\frac{dx}{k_x(x,\omega_n)} = \frac{dy}{k_y} = \frac{dz}{k_z} \tag{27}$$

with $k_x(x,\omega_n)$ defined in (23), and the frequency ω_n satisfying (24) for a given n. The projection of the ray trajectory onto the (x,y) plane is shown schematically in Figure 7*a*. The wavepacket leaves the boundary at x_m with initial wavenumber $\mathbf{k}(x_m)$. Since the wavefronts are inclined relative to $\hat{\mathbf{x}}$ the left-hand side of the wavefront experiences a larger Alfvén speed than the right-hand side, and runs ahead sightly. It is this differential velocity that causes the wavefront to rotate and the ray to bend (commonly referred to as refraction in optics textbooks). Eventually the ray is completely turned around and returns to x_m, where it is reflected as in the previous section. The ray can be thought of as being reflected at the turning point due to the nonuniformity of the medium. The position of the inner reflection point will vary for different modes. Thus the effective size of the cavity depends upon n, k_y, and k_z.

The path of the ray in Figure 7*a* may be calculated explicitly by the first two relations in (27). The point at which the ray turns around (when $k_x = 0$) is at x_t (see (21) and (23)). The Alfvén resonance will be located at a smaller x value x_r. Integrating (27) over the section of the ray path between x_t and x_m gives the distance moved in y to be Δy,

$$\Delta y = k_y \int_{x_t}^{x_m} \frac{dx}{k_x(x)} \tag{28}$$

The ray propagates at the local Alfvén speed V in the direction of $\mathbf{k}$, and the component of this velocity in the $\hat{\mathbf{x}}$ direction is $Vk_x/k \equiv V^2 k_x/\omega$ (employing (23)). Thus the time taken (Δt) for the ray to propagate from x_t to x_m is

$$\Delta t = \int_{x_t}^{x_m} \frac{\omega dx}{k_x(x)V^2(x)} \tag{29}$$

The speed at which energy is carried along the waveguide by this ray is simply $\Delta y/\Delta t$. From expressions (26), (28), and (29) we see that $\Delta y/\Delta t = V_g$, confirming the expectations of the previous subsection.

It is interesting to study the ray trajectories for different values of $\mathbf{k}$ at x_m. Suppose we choose a mode number n in x and wavenumber k_z, then consider varying the value of k_y. When we adjust k_y the two parameters frequency ω and position of the turning point x_t must change to satisfy the two conditions (21) and (24). In the appendix we show that for a monotonically decreasing Alfvén speed profile the value of x_t always increases when k_y^2 increases.

Figure 7*b* shows schematically how the ray paths of a given mode vary with k_y. The first ray has a small k_y and penetrates deep into the medium. This ray will have a small V_g as it shuffles along the waveguide very slowly. The third ray has a very large value of k_y, and consequently the turning point is very close to x_m. Since the third ray propagates approximately parallel to $\hat{\mathbf{y}}$ and is confined to the low Alfvén speed region, we would expect that $V_g(k_y) \to V(x_m)$ in the limit $k_y \to \infty$. We have confirmed this result for the dispersion diagram Figure 6 by evaluating the gradient of the curves for large k_y, and we find that the asymptotic group velocity is indeed $V(x_m)$. The second ray has an intermediate value of k_y. The speed of this ray along the guide will depend upon the details of the $V(x)$ profile, but typically the maximum group velocity is found for intermediate k_y.

Why should intermediate k_y have the largest group velocity? Intermediate k_y penetrates the high Alfvén speed region significantly (so the ray propagates quickly). Moreover, $\mathbf{k}(x_m)$ is oriented at an angle to $\hat{\mathbf{y}}$ small enough that the ray propagates out of the guide rather than across it. If we were to decrease k_y from that in the second ray, the trajectory would be more like the first ray and would tend to propagate across the guide, not along it. If k_y were increased, the path would be similar to the third ray, i.e., confined to a lower Alfvén speed region. The intermediate ray represents the optimum trade-off between propagating quickly but propagating out of the guide. The value of k_y which maximizes the group velocity may be found from setting $\partial V_g/\partial k_y \equiv \partial^2\omega_n/\partial k_y^2 = 0$. Naturally, this condition is dependent upon the choice of $V(x)$ and will be an integral equation in general.

The variation of group velocity with k_y is shown in Figure 8 for the $n = 1$ and 2 modes, which have maximum group velocities near $k_{ym} = 2.25/x_m$. Both modes asymptote to the group velocity $V_g = V(x_m) = 0.0339V_0$. This type of behavior is quite different to the uniform waveguide (of speed $V(x_m)$) of the previous section, where the group velocity increased monotonically with k_y and tended to $V(x_m)$ but

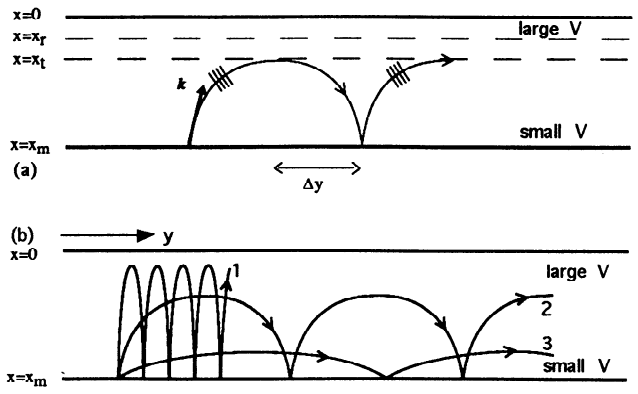

Fig. 7. (*a*) Schematic ray trajectory in the inhomogeneous waveguide. As the wavepacket propagates into the higher Alfvén speed region it refracts and has a "turning point" (at x_t) that is dependent upon n, k_z, and k_y. The position of the resonant field line for this ray (at x_r) also depends upon n, k_z, and k_y, and is located outside the propagating region $[x_t, x_m]$. (*b*) sketches of three ray paths with different values of k_y, but the same values of k_z and n.

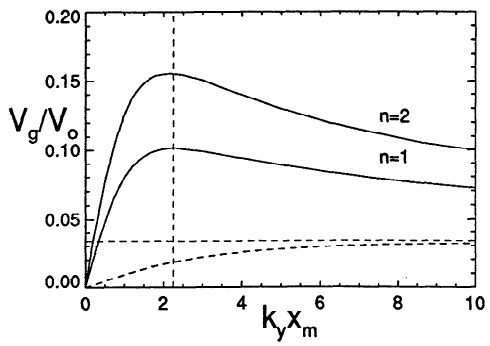

Fig. 8. Group velocity along the waveguide as a function of k_y for the inhomogeneous waveguide (solid lines). The $n = 1$ and 2 modes both have a maximum group velocity near $k_{ym} = 2.25/x_m$. For large k_y both modes have a group velocity that tends to $V(x_m) = 0.0339V_0$. A uniform waveguide (of speed $V(x_m)$) has a group velocity that increases monotonically with k_y to the speed $V(x_m)$.

never exceeded it (see (14b) and the dashed curve in Figure 8).

The dispersive properties of the inhomogeneous waveguide may be quite different to the uniform waveguide, depending upon the band of k_y modes present in the initial source disturbance. For example, if only k_y values in the band $\{0, k_{ym}\}$ are present, then both the $n = 1$ and 2 modes have dispersive properties similar to the uniform waveguide: large k_y components run ahead of small k_y components. However, if the initial source is contained in the band $\{k_{ym}, \infty\}$ we find that small k_y will travel faster than large k_y for these two modes. For a general source we expect very fine spatial structures in y ($k_y \to \infty$) to propagate down the waveguide at a speed $V(x_m)$.

6. ALFVÉN RESONANCES

In a nonuniform waveguide the fast and Alfvén modes are coupled together, and the possibility of resonant coupling must be considered. An Alfvén resonance will manifest itself as a large-amplitude ξ_y perturbation oscillating at the local Alfvén frequency. It is evident from (2) that the gradient in the $\hat{\mathbf{y}}$ direction of the magnetic pressure perturbation ($\propto b_z$) will be responsible for driving the Alfvén resonance. (The left-hand side of (2) is a simple harmonic oscillator equation for ξ_y, given k_z, and the right-hand side represents a driver.)

The discussion of fast mode propagation in the previous sections gives us some idea of the behavior of b_z along the waveguide and in time. A complete solution would include the effect of coupling to the Alfvén mode, which would enter our analysis as the phase factor α. The Alfvén resonance will absorb energy from the fast mode and cause the fast eigenfrequency and k_x to become complex - representing the temporal damping of the fast mode and the absorption of energy at x_r, respectively [*Zhu and Kivelson*, 1988]. We noted earlier that these effects are a higher-order correction to the basic WKB theory discussed above, since the resonance is situated in the evanescent tail of the fast mode.

In keeping with the lowest-order WKB solution presented in this paper we shall discuss the qualitative features of Alfvén resonances by considering b_z to be given by the dispersive notions described in section 5, and allow this pressure perturbation to drive Alfvén resonances according to (2).

Many of the concepts used in understanding resonant coupling in a cavity model are relevant to the waveguide, and we begin by reviewing the main features. In the limit k_y approaches zero x_r approaches x_t permitting the fast mode to reach the resonance without difficulty. However, as $k_y \to 0$ the gradients in the $\hat{\mathbf{y}}$ direction vanish, and there is no driving term in (2). Hence there is no resonant coupling in a cavity model when $k_y = 0$. In the opposite extreme ($k_y \to \infty$) the derivatives in y are very large; however, the separation between x_r and x_t increases, and the decay length in the evanescent tail decreases, resulting in negligible fast mode penetration to the resonance. Hence there is no resonant coupling in a cavity model when $k_y \to \infty$.

The excitation of a resonance in a waveguide is complicated by the fact that since the waves propagate down the waveguide, field lines are excited for a finite duration while the waves pass by, and not continually as in a cavity. The longer a field line is driven, the bigger will be the amplitude of the resonance [*Wright*, 1992*b*]. The time for which a certain k_y component of the source disturbance will excite a specific field line for will be of the order of $L_y/V_g(k_y)$, where L_y is the dimension of the source in the $\hat{\mathbf{y}}$ direction. Thus waves with small k_y (and so small V_g) will drive field lines for the longest time. Moreover, we saw in section 4 that the most coherent frequency a field line will experience will be corresponding to small k_y (see (17) and (18)). Although small k_y means small gradients along $\hat{\mathbf{y}}$, only these waves will provide a coherent driver for Alfvén resonances and also have the advantage of being able to drive a field line over an extended period of time. For these reasons it seems likely that a waveguide will excite Alfvén resonances at frequencies approximately equal to the eigenfrequency of the $k_y = 0$ waveguide modes. Note also from Figure 6 that ω_n is relatively insensitive to k_y for small wavenumbers ($\partial\omega_n/\partial k_y = 0$ at $k_y = 0$), so the waveguide modes in a fairly broad band around $k_y = 0$ may all act together to drive a single resonance.

7. DISCUSSION AND SUMMARY

In the preceding sections we have shown how dispersion in MHD waveguides will, after an initial phase, be able to select a steady periodic wave that will be suitable for driving a resonance. The frequency of this driver will be approximately $\omega_n(k_y = 0)$, will have a small value of k_y, and will be able to drive a single field line for an extended period of time as it has a small group velocity along the waveguide. Waveguide modes with a larger value of k_y (and V_g) will propagate down the guide more quickly and may only drive field lines for perhaps one or two cycles, resulting in no clear resonant signature.

As the small k_y components shuffle slowly down the waveguide they will lose energy to the Alfvén resonance and decrease in amplitude. Consequently, these components will drive a resonance of smaller and smaller amplitude as they move down the waveguide. This effect is compounded by fact that at any given time the field lines further away from the source region will have been driven for a shorter time, and so resonances will not have had as much time to grow as resonances on field lines near the source region.

In summary, given a source region of fast modes in a nonuniform waveguide we expect the following qualitative features: (1) The source waves disperse; intermediate and large k_y components will run down the waveguide ahead of

the small k_y components that linger near the source region. (2) The small k_y band of components will provide a steady periodic driver for Alfvén resonances at frequencies given approximately by $\omega_n(k_y = 0)$. (3) The small k_y band will propagate very slowly down the waveguide, decaying in time. Thus the largest Alfvén resonances will occur near the source region.

The features discussed above need to be examined quantitatively by numerical and analytical studies which will model the wave coupling process in detail and will be the subject of a future paper. Finally, we note that waveguide dispersion provides a complementary mechanism to that of *Walker et al.* [1992] by which a suitable resonant driver may be established. If the magnetospheric waveguide extends out to the bow shock, as suggested by *Harrold and Samson* [1992], we believe that the waveguide dispersion model described here will be the more relevant mechanism for exciting Alfvén resonances.

APPENDIX

In this appendix we examine how the turning point x_t changes with k_y. Suppose we have an initial solution to (21) and (24), say, k_{y0}, ω_0 and x_{t0}. We now introduce a change in k_y of δk_y which generates perturbations $\delta\omega$ and δx_t - we assume k_z to be constant. Collecting linear term in δ from an expansion of (26) gives

$$\delta\omega\omega_0\langle V^{-2}\rangle_{x_{t0}}^{x_m} = k_{y0}\delta k_y \qquad \text{(A1)}$$

so we know the change in eigenfrequency in terms of δk_y. Note that increasing the size of k_y means the size of the eigenfrequency increases.

The Alfvén speed may be expanded as a Taylor series about the original turning point,

$$V^2(x_{t0} + \delta x_t) = V^2(x_{t0}) + \delta x_t V^{2\prime}(x_{t0}) \qquad \text{(A2)}$$

where the prime denotes differentiation with respect to x. If ω and k are known (21) defines the position of the turning point. Substituition of (A2) in (21) yields

$$\delta x_t = \frac{2\omega_0\delta\omega - 2k_{y0}\delta k_y V^2(x_{t0})}{\left(k_{y0}^2 + k_z^2\right) V^{2\prime}(x_{t0})} \qquad \text{(A3)}$$

Eliminating δk_y in favour of $\delta\omega$ with (A1) the above equation becomes

$$\delta x_t = \frac{2\omega_0\delta\omega}{\left(k_{y0}^2 + k_z^2\right) V^{2\prime}(x_{t0})} \cdot \left[1 - V^2(x_{t0})\langle V^{-2}\rangle\right] \qquad \text{(A4)}$$

where we have omitted the cumbersome limits on the integral. Explicitly, the second term in the square brackets is

$$V^2(x_{t0})\langle V^{-2}\rangle = \int_{x_{t0}}^{x_m} \frac{1}{k_x}\frac{V^2(x_{t0})}{V^2}\mathrm{d}x \Big/ \int_{x_{t0}}^{x_m} \frac{1}{k_x}\mathrm{d}x \qquad \text{(A5)}$$

Recall that we are assuming the Alfvén speed to decrease monotonically with x; thus $V^2(x_{t0})/V^2(x) \geq 1$ on the integration interval x_{t0} to x_m, and $V^{2\prime} < 0$. Under these conditions (A4) states that δx_t is always positive for k_y^2 increasing , i.e., the turning point x_t moves closer to the outer boundary x_m.

Acknowledgments. This work was carried out while the author was supported by a UK SERC Advanced Fellowship.

The Editor thanks B. G. R. Harrold and X. Zhu for their assistance in evaluating this paper.

REFERENCES

Allan, W., S. P. White, and E. M. Poulter, Impulse-excited hydromagnetic cavity and field-line resonances in the magnetosphere, *Planet. Space Sci., 34,* 371, 1986.

Barston, E. M., Electrostatic oscillations in inhomogeneous cold plasmas, *Ann. Phys. (N.Y.), 29,* 282, 1964.

Bender, C. M., and S. A. Orszag, *Advanced Mathematical Methods for Scientists and Engineers,* McGraw-Hill, New York, 1978.

Chen, L., and A. Hasegawa, A theory of long-period magnetic pulsations 1. Steady state excitation of field line resonance, *J. Geophys. Res., 79,* 1024, 1974.

Dungey, J. W., Electrodynamics of the outer atmosphere, *Sci. Rep. 69,* Penn. State Univ., University Park, 1954.

Dungey, J. W., Hydromagnetic waves, in *Physics of Geomagnetic Phenomena,* vol. 2, edited by S. Matsushita and W. H. Campbell, pp. 913–934, Academic, San Diego, Calif., 1967.

Harrold, B. G., and J. C. Samson, Standing ULF modes of the magnetosphere: A theory, *Geophys. Res. Lett., 19,* 1811, 1992.

Inhester, B., Numerical modeling of hydromagnetic wave coupling in the magnetosphere, *J. Geophys. Res., 92,* 4751, 1987.

Kivelson, M. G., and D. J. Southwood, Resonant ULF waves: A new interpretation, *Geophys. Res. Lett., 12,* 49, 1985.

Kivelson, M. G., and D. J. Southwood, Coupling of global magnetospheric MHD eigenmodes to field line resonances, *J. Geophys. Res., 91,* 4345, 1986.

Lee, D. H., and R. L. Lysak, Magnetospheric ULF wave coupling in the dipole model: The impulsive excitation, *J. Geophys. Res., 94,* 17,097, 1989.

Samson, J. C., B. G. Harrold, J. M. Ruohoniemi, and A. D. M. Walker, Field line resonances associated with MHD waveguides in the magnetosphere, *Geophys. Res. Lett., 19,* 441, 1992.

Southwood, D. J., Some features of field line resonances in the magnetosphere, *Planet. Space Sci., 22,* 483, 1974.

Walker, A. D. M., J. M. Ruohoniemi, K. B. Baker, and R. A. Greenwald, Spatial and temporal behavior of ULF pulsations observed by the Goose Bay HF radar, *J. Geophys. Res., 97,* 12,187, 1992.

Wright, A. N., Coupling of fast and Alfvén modes in realistic magnetospheric geometries, *J. Geophys. Res., 97,* 6429, 1992*a*.

Wright, A. N., Asymptotic and time-dependent solutions of magnetic pulsations in realistic magnetic field geometries, *J. Geophys. Res., 97,* 6439, 1992*b*.

Zhu, X., and M. G. Kivelson, Analytic formulation and quantitative solutions of the coupled ULF wave problem, *J. Geophys. Res., 93,* 8602, 1988.

A. N. Wright, Department of Mathematical and Computational Sciences, University of St. Andrews, St. Andrews, Fife KY16 9SS, Scotland, U.K.

(Received June 30, 1993; revised June 30, 1993; accepted July 28, 1993.)